AIP | Physics of Fluids

Energy dissipation and resolution of steep gradients in one-dimensional Burgers flows

Chuong V. Tran and David G. Dritschel

Citation: Physics of Fluids (1994-present) **22**, 037102 (2010); doi: 10.1063/1.3327284
View online: http://dx.doi.org/10.1063/1.3327284
View Table of Contents: http://scitation.aip.org/content/aip/journal/pof2/22/3?ver=pdfcov
Published by the AIP Publishing

Energy dissipation and resolution of steep gradients in one-dimensional Burgers flows

Chuong V. Tran and David G. Dritschel
School of Mathematics and Statistics, University of St Andrews, St Andrews KY16 9SS, United Kingdom

(Received 12 October 2009; accepted 13 January 2010; published online 19 March 2010)

Traveling-wave solutions of the inviscid Burgers equation having smooth initial wave profiles of suitable shapes are known to develop shocks (infinite gradients) in finite times. Such singular solutions are characterized by energy spectra that scale with the wave number k as k^{-2}. In the presence of viscosity $\nu>0$, no shocks can develop, and smooth solutions remain so for all times $t>0$, eventually decaying to zero as $t\to\infty$. At peak energy dissipation, say $t=t_*$, the spectrum of such a smooth solution extends to a finite dissipation wave number k_ν and falls off more rapidly, presumably exponentially, for $k>k_\nu$. The number N of Fourier modes within the so-called inertial range is proportional to k_ν. This represents the number of modes necessary to resolve the dissipation scale and can be thought of as the system's number of degrees of freedom. The peak energy dissipation rate ϵ remains positive and becomes independent of ν in the inviscid limit. In this study, we carry out an analysis which verifies the dynamical features described above and derive upper bounds for ϵ and N. It is found that ϵ satisfies $\epsilon\le\nu^{2\alpha-1}\|u_*\|_\infty^{2(1-\alpha)}\|(-\Delta)^{\alpha/2}u_*\|^2$, where $\alpha<1$ and $u_*=u(x,t_*)$ is the velocity field at $t=t_*$. Given $\epsilon>0$ in the limit $\nu\to 0$, this implies that the energy spectrum remains no steeper than k^{-2} in that limit. For the critical k^{-2} scaling, the bound for ϵ reduces to $\epsilon\le\sqrt{3}k_0\|u_0\|_\infty\|u_0\|^2$, where k_0 marks the lower end of the inertial range and $u_0=u(x,0)$. This implies $N\le\sqrt{3}L\|u_0\|_\infty/\nu$, where L is the domain size, which is shown to coincide with a rigorous estimate for the number of degrees of freedom defined in terms of local Lyapunov exponents. We demonstrate both analytically and numerically an instance, where the k^{-2} scaling is uniquely realizable. The numerics also return ϵ and t_*, consistent with analytic values derived from the corresponding limiting weak solution. *© 2010 American Institute of Physics*.
[doi:10.1063/1.3327284]

I. INTRODUCTION

In 1948, Burgers[1] introduced the equation

$$u_t+uu_x=\nu u_{xx}, \tag{1}$$

as a model for fluid turbulence. Here, $u(x,t)$ is a one-dimensional velocity field and $\nu>0$ plays the role of viscosity in a usual fluid. On the one hand, this model captures the two most fundamental features of fluid dynamics by its quadratic advection and viscosity terms. On the other hand, Eq. (1) lacks a pressure term, thus governing a hypothetical compressible fluid without pressure. The absence of a pressure-like term makes Eq. (1) integrable by the Cole–Hopf method.[2,3] This renders Eq. (1) and its generalization to higher dimensions poor models for fluid turbulence. Despite this apparent shortcoming, the Burgers equation has been widely studied for a variety of applications.[4–13]

The development of shock waves or discontinuities (infinite gradients) from suitable smooth initial velocity profiles is an intrinsic property of the inviscid Burgers equation. Given a differentiable initial profile $u(x,0)=u_0(x)$, Eq. (1) with $\nu=0$ is implicitly solved by the traveling-wave solution

$$u(x,t)=u_0(\xi)=u_0(x-ut). \tag{2}$$

By taking the spatial derivative of Eq. (2) and solving the resulting equation for u_x one obtains

$$u_x=\frac{u_0'}{1+tu_0'}, \tag{3}$$

where $u_0'(\xi)$ denotes the derivative of $u_0(\xi)$. It follows that u_x diverges ($u_x\to-\infty$) provided that $u_0'(\xi)<0$ for some ξ. The earliest time $t=T$ for this to occur is $T=-1/u_0'(x_0)$, where $u_0'(x_0)$ is the steepest slope of $u_0(x)$ occurring at $x=x_0$. This steepest slope travels at the speed $u_0(x_0)$ and gets ever steeper as $t\to T$, becoming infinitely steep when $t=T$ at $x=x_0+u_0(x_0)T=x_0-u_0(x_0)/u_0'(x_0)$. In summary, the space-time coordinate of the shock is

$$(x,t)=\left(x_0-\frac{u_0(x_0)}{u_0'(x_0)},\frac{-1}{u_0'(x_0)}\right). \tag{4}$$

Such a singular solution is characterized by an energy spectrum $E(k)$ that scales with the wave number k as $E(k)\propto k^{-2}$, which is the spectrum of a step function.

Under the effects of viscosity, the shock is suppressed, and the solution remains smooth and decays to zero in the limit $t\to\infty$. This statement is true however small the viscosity. This means that the maximally achievable (peak) energy dissipation rate, hereafter denoted by ϵ_m, remains positive in the inviscid limit $\nu\to 0$. For fixed $\nu>0$, the velocity gradient $|u_x|$ can achieve a finite maximum only. Presumably, the corresponding energy spectrum would retain the k^{-2} scaling up to a finite dissipation wave number k_ν, around which the dissipation of energy mainly takes place and beyond which a more rapid decay, probably exponential decay, occurs. Given this scaling, ϵ_m scales as νk_ν. It follows that the number N of Fourier modes within the wave number range $k \le k_\nu$, the so-called inertial range is

$$N \propto k_\nu \propto \frac{\epsilon_m}{\nu}, \tag{5}$$

for dimensionally appropriate proportionality constants. This is the number of modes necessary to resolve the dissipation scale and can be considered the system's number of degrees of freedom.

In this study, we carry out an analysis that quantitatively confirms the dynamical features described above. It is found that ϵ_m satisfies

$$\epsilon_m \le \nu^{2\alpha-1}\|u_*\|_\infty^{2(1-\alpha)}\|(-\Delta)^{\alpha/2}u_*\|^2, \tag{6}$$

where $\alpha<1$, Δ is the Laplace operator, $u_*=u(x,t_*)$ is the velocity field at the time of peak energy dissipation $t=t_*$, and $\|\cdot\|_\infty$ and $\|\cdot\|$ denote L^∞ and L^2 norms, respectively. Given that $\epsilon_m>0$ in the limit $\nu\to 0$, this result implies that the energy spectrum $E(k,t_*)$ becomes no steeper than k^{-2} in that limit. For this critical scaling, ϵ_m is found to satisfy $\epsilon_m \le \sqrt{3}k_0\|u_*\|_\infty\|u_*\|^2 \le \sqrt{3}k_0\|u_0\|_\infty\|u_0\|^2$, where $u_0=u(x,0)$ and k_0 is the wave number that marks the lower end of the energy inertial range. This result further implies $k_\nu \le \sqrt{3}\|u_0\|_\infty/\nu$. It follows that $N\le \sqrt{3}L\|u_0\|_\infty/\nu$, where L is the domain size, which is shown to coincide with a rigorous estimate for the number of degrees of freedom defined in terms of local Lyapunov exponents. Note that one can identify the upper bound for N with the Reynolds number Re as in the case of a real fluid. Thus, the system's number of degrees of freedom scales linearly with Re. We demonstrate both mathematically and numerically an instance where $E(k,t_*)\propto k^{-2}$ is uniquely realizable. The numerics also return the values of ϵ_m and t_*, which are consistent with those derived from the corresponding limiting weak solution.

II. ENERGY DISSIPATION AND DISSIPATION WAVE NUMBER

For simplicity, we consider periodic solutions of Eq. (1) having period $2\pi L$ and vanishing spatial average. The usual L^p norm of u (and of its derivatives), for all $p>0$ including $p=\infty$, is defined by $\|u\|_p=\langle |u|^p\rangle^{1/p}$, where $\langle\cdot\rangle$ denotes a domain average. The advection term of the Burgers equation conserves $\|u\|_p$. Under viscous effects, $\|u\|_p$ decays for $p\ge 1$ and is governed by

$$\frac{d}{dt}\|u\|_p = -\nu(p-1)\|u\|_p^{1-p}\langle |u|^{p-2}u_x^2\rangle. \tag{7}$$

Since we are dealing with L^2 and L^∞ norms only, we omit the subscript $p=2$ in the former for convenience. The decay of the energy $\|u\|^2/2$ is governed by

$$\frac{1}{2}\frac{d}{dt}\|u\|^2 = -\nu\|u_x\|^2. \tag{8}$$

This section is mainly interested in optimal estimates for the decay rate $\nu\|u_x\|^2$, particularly in the limit of small ν, and related issues concerning the energy inertial range.

The governing equation for the velocity gradient u_x is

$$u_{xt} + uu_{xx} + u_x^2 = \nu u_{xxx}. \tag{9}$$

By multiplying Eq. (1) by u_{xx} [or Eq. (9) by u_x] and integrating the resulting equation over the domain we obtain the evolution equation for the mean-square velocity gradient $\|u_x\|^2$,

$$\begin{aligned}\frac{1}{2}\frac{d}{dt}\|u_x\|^2 &= \langle u_{xx}uu_x\rangle - \nu\|u_{xx}\|^2 \le \|u\|_\infty\|u_x\|\|u_{xx}\| - \nu\|u_{xx}\|^2 \\ &= \frac{\|u_{xx}\|^2}{\|u_x\|^2}\left(\|u\|_\infty\frac{\|u_x\|^3}{\|u_{xx}\|} - \nu\|u_x\|^2\right),\end{aligned} \tag{10}$$

where the inequality is straightforward. The final line of Eq. (10) can be used to derive an upper bound for the energy dissipation rate $\nu\|u_x\|^2$. For this purpose, consider the inequality [see Eq. (7) of Ref. 14]

$$\frac{\|u_x\|^3}{\|u_{xx}\|} \le \frac{\|(-\Delta)^{\alpha/2}u\|^{1/(1-\alpha)}}{\|u_x\|^{(2\alpha-1)/(1-\alpha)}}, \tag{11}$$

where $\alpha<1$ is a parameter, which can be varied for an optimal bound, and Δ is the Laplace operator. The fractional derivative $(-\Delta)^{\alpha/2}$ is a positive operator and is defined by $\widehat{(-\Delta)^{\alpha/2}u}=k^\alpha\hat{u}$, where $\widehat{(-\Delta)^{\alpha/2}u}$ and $\hat{u}$ are the Fourier transforms of $(-\Delta)^{\alpha/2}u$ and u, respectively. Upon substituting Eq. (11) into Eq. (10) and noting that $d\|u_x\|^2/dt=0$ at the time of peak energy dissipation $t=t_*$, we can deduce that

$$\epsilon_m \le \nu^{2\alpha-1}\|u_*\|_\infty^{2(1-\alpha)}\|(-\Delta)^{\alpha/2}u_*\|^2, \tag{12}$$

where $\|u_*\|_\infty$ is bounded by its initial value, but $\|(-\Delta)^{\alpha/2}u_*\|$ can be large, depending on both $E(k,t_*)$ and α. In Sec. IV, we demonstrate both analytically and numerically that in the limit $\nu\to 0$, t^* is independent of ν and, in general, not related to the singularity time T of the corresponding inviscid solution.

Equation (12) confirms the fact that $\epsilon_m<\infty$ (and hence $\|u_x\|<\infty$) for $\nu>0$ as one can set $\alpha=0$ and obtain $\epsilon_m\le\|u_*\|_\infty^2\|u_*\|^2/\nu\le\|u_0\|_\infty^2\|u_0\|^2/\nu$. This bound can be highly excessive, and a more optimal estimate is possible by varying the "optimization" parameter α within the permissible range $\alpha<1$. Observe that the spectrum of $\|(-\Delta)^{\alpha/2}u\|^2/2$ is $k^{2\alpha}E(k)$. So, if the energy spectrum $E(k,t_*)$ is strictly steeper than k^{-2}, then $\|(-\Delta)^{\alpha/2}u_*\|$ is bounded for some $\alpha>1/2$. If this were the case for all ν, including the limit $\nu\to 0$, then the upper bound for ϵ_m in Eq. (12) would vanish, thereby contradicting the fact that $\epsilon_m>0$ in that limit. This rules out energy spectra steeper than k^{-2}. In Sec. IV, we mathematically demonstrate an instance where energy spectra shallower than k^{-2} are also ruled out. Thus the scaling k^{-2} is uniquely realizable. This suggests that in general, the most plausible scenario is that in the inviscid limit, $E(k,t_*)$ approaches the k^{-2} critical scaling.

Now, suppose that $E(k)=Ck^{-2}/2$, for $k\in[k_0,k_\nu]$, where $C>0$ is a constant. Note that k_0 is not necessarily the lowest wave number $1/L$. We then have $\|u\|^2 = C\int_{k_0}^{k_\nu} k^{-2}dk$, so $C = k_0\|u\|^2$. Thus, $E(k) = k_0\|u\|^2 k^{-2}/2$. For this case, a direct estimate of the ratio $\|u_x\|^3/\|u_{xx}\|$ is

$$\frac{\|u_x\|^3}{\|u_{xx}\|} = \sqrt{3}k_0\|u\|^2. \tag{13}$$

By applying this equation to u_* and substituting the resulting estimate into Eq. (10), we deduce the upper bound

$$\epsilon_m \le \sqrt{3}k_0\|u_*\|_\infty\|u_*\|^2 \le \sqrt{3}k_0\|u_0\|_\infty\|u_0\|^2. \tag{14}$$

We find later by an example for the parameter values $\|u_0\|_\infty = 1$, $\|u_0\|^2 = 1/2$, and $k_0 = 1$ that $\epsilon_m = 0.1061$, which gives us a sense of the sharpness of the derived upper bound $\sqrt{3}k_0\|u_0\|_\infty\|u_0\|^2 = \sqrt{3}/2$. The dissipation wave number k_ν, which marks the end of the k^{-2} inertial range is found to satisfy

$$k_\nu \le \frac{\sqrt{3}\|u_0\|_\infty}{\nu}. \tag{15}$$

It follows that the number N of Fourier modes within this inertial range is bounded by

$$N \le \frac{\sqrt{3}L\|u_0\|_\infty}{\nu} = \mathrm{Re}, \tag{16}$$

where Re is the Reynolds number. Note that this estimate also includes the modes corresponding to $k < k_0$. The linear dependence of N on Re is interesting and is rigorously verified, without reference to $E(k,t_*)$ in what follows.

III. LYAPUNOV EXPONENTS AND NUMBER OF DEGREES OF FREEDOM

This section derives a rigorous estimate for the number of degrees of freedom, which is defined as the minimum number of greatest local Lyapunov exponents (of a general trajectory in phase space) whose sum becomes negative. This number, denoted by D, is the dimension of the linear space (spanned by the corresponding Lyapunov vectors), which can adequately "accommodate" the solution locally, and is essentially the so-called Lyapunov or Kaplan–Yorke dimension.[15,16] Its estimate is found to agree with that for N obtained earlier in Sec. II. This agreement is not coincidental and can be considered as analytic evidence for the expected k^{-2} energy spectrum used in the estimation of N. Like N, D can be thought of as the number of Fourier modes necessary to resolve the steepest velocity gradient during the course of evolution, particularly around $t = t_*$. We follow the procedure formulated by Tran and Blackbourn[17] in the calculation of the number of degrees of freedom for two-dimensional Navier–Stokes turbulence. For a detailed discussion of the significance of D, see Refs. 17 and 18 and references therein.

Given the solution $u(x,t)$ starting from some smooth initial velocity field $u_0(x)$, consider a disturbance $v(x,t)$ satisfying the same conditions as $u(x,t)$, i.e., periodic boundary condition and zero spatial average. The linear evolution of $v(x,t)$ is governed by

$$v_t + uv_x + vu_x = \nu v_{xx}. \tag{17}$$

The governing equation for the norm $\|v\|$ is

$$\begin{aligned}\|v\|\frac{d}{dt}\|v\| &= -\langle v(uv_x + vu_x)\rangle - \nu\|v_x\|^2\\ &= \langle uvv_x\rangle - \nu\|v_x\|^2 \le \|u\|_\infty\|v\|\|v_x\| - \nu\|v_x\|^2\\ &\le \|u_0\|_\infty\|v\|\|v_x\| - \nu\|v_x\|^2,\end{aligned} \tag{18}$$

where we have used $\langle v^2u_x\rangle = -2\langle uvv_x\rangle$ by integration by parts and the inequalities are straightforward. Dividing both sides of Eq. (18) by $\|v\|^2$ yields

$$\lambda = \frac{1}{\|v\|}\frac{d}{dt}\|v\| \le \|u_0\|_\infty\frac{\|v_x\|}{\|v\|} - \nu\frac{\|v_x\|^2}{\|v\|^2}, \tag{19}$$

where λ is the exponential rate of growth ($\lambda > 0$) or decay ($\lambda < 0$) of the disturbance norm $\|v\|$.

The set of n greatest local Lyapunov exponents $\{\lambda_1, \lambda_2, \ldots, \lambda_n\}$ and the corresponding orthonormal set of n most unstable disturbances $\{v^1, v^2, \ldots, v^n\}$ can be derived by successively maximizing λ with respect to all admissible disturbances v subject to the following orthogonality constraint. At each step i in the process, the maximizer v is required to satisfy both $\|v\| = 1$ and $\langle vv^j\rangle = 0$, for $j = 1, 2, \ldots, i-1$, where v^j is the solution obtained at the jth step. Since each normalized solution (λ_i, v^i) satisfies Eq. (19), we have

$$\begin{aligned}\sum_{i=1}^n \lambda_i &\le \|u_0\|_\infty\sum_{i=1}^n \|v_x^i\| - \nu\sum_{i=1}^n \|v_x^i\|^2\\ &\le \|u_0\|_\infty\left(n\sum_{i=1}^n \|v_x^i\|^2\right)^{1/2} - \nu\sum_{i=1}^n \|v_x^i\|^2\\ &= \left(\sum_{i=1}^n \|v_x^i\|^2\right)^{1/2}\left(\|u_0\|_\infty n^{1/2} - \nu\left(\sum_{i=1}^n \|v_x^i\|^2\right)^{1/2}\right)\\ &\le \left(n\sum_{i=1}^n \|v_x^i\|^2\right)^{1/2}\left(\|u_0\|_\infty - \frac{\nu n}{cL}\right),\end{aligned} \tag{20}$$

where c is a constant independent of the orthonormal set in question. In Eq. (20), we have applied the Cauchy–Schwarz inequality $\sum_{i=1}^n\|v_x^i\| \le (n\sum_{i=1}^n\|v_x^i\|^2)^{1/2}$ and used the estimate

$$\sum_{i=1}^n \|v_x^i\|^2 \ge \frac{n^3}{c^2L^2}, \tag{21}$$

which is a consequence of the Rayleigh–Ritz principle. By this principle, the left-hand side of Eq. (21) is not smaller than the sum of the first (i.e., smallest) n eigenvalues of $-\Delta$. These eigenvalues are $1/L^2, 2^2/L^2, \ldots, n^2/L^2$ and sum up to $n(n+1)(2n+1)/(6L^2)$. Hence, Eq. (21) follows with c tending to $\sqrt{3}$ for large n. Now the condition $\sum_{i=1}^n\lambda_i \le 0$ is satisfied when $n \ge cL\|u_0\|_\infty/\nu$. It follows that

$$D \le c\frac{L\|u_0\|_\infty}{\nu}. \tag{22}$$

This estimate agrees with the upper bound (16) for N, which was derived by assuming the energy spectrum $E(k) \propto k^{-2}$.

This agreement provides us with confidence in the plausibility of the k^{-2} scaling.

The term on the right-hand side of Eq. (22) is the Reynolds number Re defined earlier with $c=\sqrt{3}$. Thus D scales linearly with Re. For a comparison, D scales as $\mathrm{Re}(1+\ln \mathrm{Re})^{1/3}$ and $\mathrm{Re}^{9/4}$ for two-dimensional and three-dimensional turbulence, respectively. The former has recently been derived,[17] while the latter is a classical result deduced from the Kolmogorov theory. These scalings reflect the intrinsic characteristics that the dynamics of the two-dimensional vorticity gradient and three-dimensional vorticity are effectively linear and quadratically nonlinear, respectively.[18,19] The present finding of an exactly linear dependence of D on Re is somewhat unexpected as the Burgers velocity gradient dynamics are quadratically nonlinear, just as in three-dimensional vorticity dynamics. Nonetheless, this is not a total surprise if the dimension of the physical space, which plays a significant role in the scaling of D with Re, is taken into account.[18] Note that in all three cases, D scales linearly with the domain volume, given all else is fixed. This is in accord with the notion of extensive chaos.[20–22] The linear scaling of D with Re for the Burgers case is fully justified in the numerical simulations reported in Sec. IV, where we observe that the ratio D/Re is best kept fixed (at order unity) for various resolutions. Hence, doubling the resolution (i.e., doubling D) allows the viscosity to be halved, given all else is fixed. This allows the exponential dissipation rate νk^2 at the truncation wave number to grow as Re. On the other hand, this same linear scaling of D with Re in two-dimensional turbulence means that numerical simulations can be performed using a fixed dissipation rate νk^2 at the truncation wave number, for different resolutions. Thus, doubling the resolution (i.e., quadrupling D) allows the viscosity to be reduced by a factor of 4. This fact is well known to numerical analysts. The scaling of D as $\mathrm{Re}^{9/4}$ in three-dimensional turbulence implies that the dissipation rate νk^2 at the truncation wave number should be proportional to $\mathrm{Re}^{1/2}$. This means that doubling the resolution (i.e., octupling D) allows the viscosity to be reduced by at most $2^{-4/3}$.

IV. A CASE STUDY

In this section, we analytically and numerically consider an example that confirms the results derived in the preceding sections. In addition, we prove that no power-law energy spectra other than k^{-2} are realizable, thus giving an exact result of the slope of $E(k,t_*)$ rather than a constraint for this particular case. We also determine by numerical simulations the viscosity-independent maximum dissipation rate ϵ_m and the corresponding time $t=t_*$ when this occurs. The numerical values of these dynamical parameters agree with those derived from the corresponding limiting weak solution.

A. Analytical consideration

We consider the periodic domain $[-\pi,\pi]$, i.e., $L=1$, and $u_0(x)=-\sin x$. This initial profile was used in a computational study[13] of the Burgers equation, using 4096 grid points. In the next subsection, we report results from simulations using up to 4×10^4 Fourier modes. It can be readily seen that Eq.

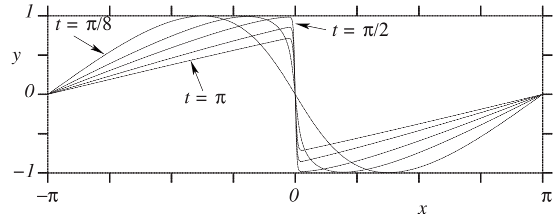

FIG. 1. A viscous solution to Burgers equation starting from $u(x,0)=-\sin x$, for $\nu=0.02$, and shown at times $t=\pi/8$, $5\pi/16\approx 1$, $\pi/2$, $3\pi/4$, and π.

(1) admits odd functions as solutions. In other words, if $f(x,t)$ is a solution, then $f(-x,t)$ is also a solution provided that $f(x,t)=-f(-x,t)$. Hence, for the initial profile under consideration, $u(x,t)$ remains odd for all $t>0$. We can then express $u(x,t)$ in terms of an odd Fourier series

$$u(x,t)=\sum_k u_k(t)\sin kx, \tag{23}$$

where $k=1,2,3,\cdots$ are the wave numbers. The gradient u_x is given by

$$u_x(x,t)=\sum_k k u_k(t)\cos kx. \tag{24}$$

The origin is "stationary" and has the steepest negative slope, initially equalling -1, which is given in terms of u_k by

$$u_x(0,t)=\sum_k k u_k(t). \tag{25}$$

The third derivative $u_{xxx}(0,t)$ is

$$u_{xxx}(0,t)=-\sum_k k^3 u_k(t). \tag{26}$$

By substituting Eqs. (25) and (26) into Eq. (9), one obtains

$$\frac{\partial}{\partial t}\sum_k k u_k=-\left(\sum_k k u_k\right)^2-\nu\sum_k k^3 u_k. \tag{27}$$

In the inviscid case, $u_x(0,t)\to-\infty$ as $t\to T=1$. This can be seen either by solving Eq. (27) with $\nu=0$ or directly from Eq. (4). Figure 1 illustrates the viscous solution (for $\nu=0.02$) at a few selected times before, near and after the inviscid singularity time ($t=1$).

The evolution of the Fourier coefficients $u_k(t)$ is governed by

$$\frac{\partial}{\partial t}u_k=\frac{k}{4}u_{k/2}^2\mp\frac{k}{2}\sum_{m\pm\ell=k}u_m u_\ell-\nu k^2 u_k, \tag{28}$$

where the sum is over all pairs of wave numbers m and ℓ, including $m=\ell=k/2$ when k is even, satisfying the triad condition $m\pm\ell=k$. Within each individual wave number triad, the energy is conservatively transferred from each of the two lower wave numbers to the third and higher wave number or vice versa. It can be seen that all wave numbers are initially excited in such a way that $u_k<0$. Plausibly, no particular modes would become completely depleted of energy during the subsequent evolution. This means that u_k does not change sign and remains negative. This fact is verified below in the

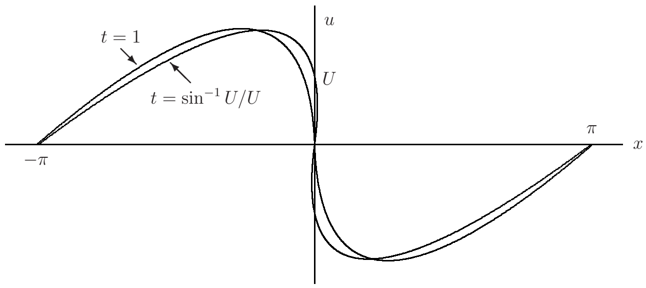

FIG. 2. A schematic description of energy loss after wave breaking at $t=1$ for the traveling-wave solution $u=-\sin(x-ut)$ of the inviscid Burgers equation. The energy dissipation rate is $U^3(t)/(3\pi)$, where $2U(t)$ is the shock width. This rate is zero upon wave breaking and grows to its maximum of $1/(3\pi)$ at $t=\pi/2$.

numerical simulations. As a consequence, the transfer of energy to ever-smaller scales is irreversible, and each Fourier mode contributes to the steepness of the slope $u_x(0,t)$ as there are no cancellations in the sum $\Sigma_k k u_k$. The nonlinearity can be said to operate at "full strength," without "depletion." This is consistent with the fact that $u_x(0,t)$ quickly diverges if $\nu=0$; indeed $u_x(0,1)=-\infty$. This observation prompts us to take $u_k<0$ for all k in what follows.

Consider the inertial range scaling $u_k=-c_\gamma k^{-\gamma}$, for $0<\gamma<3/2$ and $c_\gamma>0$, which corresponds to the energy spectrum $E(k)=c_\gamma^2 k^{-2\gamma}/2$. By substituting this scaling for u_k into the right-hand side of Eq. (27) we obtain

$$\frac{\partial}{\partial t}\sum_k k u_k = -\frac{c_\gamma^2 k_\nu^{4-2\gamma}}{(2-\gamma)^2} + \nu\frac{c_\gamma k_\nu^{4-\gamma}}{4-\gamma} = k_\nu^{1+\gamma}\left(\frac{(3-2\gamma)\epsilon_m}{c_\gamma(4-\gamma)} - \frac{c_\gamma^2 k_\nu^{3-3\gamma}}{(2-\gamma)^2}\right), \tag{29}$$

where $\epsilon_m=\nu c_\gamma^2 k_\nu^{3-2\gamma}/(3-2\gamma)$ has been calculated from the above spectrum. The fact that both $\Sigma_k k u_k \to -\infty$ and $0<\epsilon_m<\infty$ as $k_\nu\to\infty$ requires $\gamma=1$, which is the only possibility allowed by Eq. (29). Indeed, if $\gamma>1$ (which has already been ruled out in general), then the second term in the brackets of Eq. (29) could be made arbitrarily small for sufficiently large k_ν and the right-hand side would become positive. This contradicts the fact that $\Sigma_k k u_k\to-\infty$. On the other hand, if $\gamma<1$, then the second term in the brackets of Eq. (29) could be made arbitrarily large for sufficiently large k_ν and the right-hand side would become negative. The gradient at the origin $\Sigma_k k u_k$ would diverge for $k_\nu<\infty$, which is not possible.

We now consider the energy dissipation rate in the inviscid case due to the lack of smoothness of solution after wave breaking at $t=1$. This consideration allows us to determine the energy dissipation rate, among other things, of the viscous case in the inviscid limit. For $t>1$, the traveling-wave solution becomes multivalued in a neighborhood of $x=0$ as the respective portions $u>0$ and $u<0$ of u cross over the vertical axis, invading the region $x>0$ and $x<0$ (see Fig. 2). Consider the weak solution consisting of two disconnected traveling-wave branches $u_+(x,t)$ and $u_-(x,t)$ given by

$$u_+(x,t) = \begin{cases} -\sin(x-u_+t) & \text{for } -\pi\le x\le 0, \\ 0 & \text{for } 0<x\le\pi, \end{cases} \tag{30}$$

and

$$u_-(x,t) = \begin{cases} -\sin(x-u_-t) & \text{for } 0\le x\le \pi, \\ 0 & \text{for } -\pi\le x<0. \end{cases} \tag{31}$$

These terminate on the vertical axis at $u_+(0,t)=U(t)$ and $u_-(0,t)=-U(t)$, where the (half) shock width $U(t)$ is given implicitly by $U=\sin(Ut)$. Evidently, $\lim_{t\to 1_+} U(t)=0$ and $U(\pi/2)=1$, the latter of which is the global maximum. The evolution of the energy corresponding to this solution is governed by

$$\frac{1}{2}\frac{d}{dt}\|u\|^2 = -\frac{1}{2\pi}\left[\int_{-\pi}^{0} u_+^2(u_+)_x dx + \int_0^{\pi} u_-^2(u_-)_x dx\right] = -\frac{1}{6\pi}\left[\int_{-\pi}^{0}(u_+^3)_x dx + \int_0^{\pi}(u_-^3)_x dx\right] = -\frac{U^3}{3\pi}. \tag{32}$$

The energy dissipation rate $U^3/(3\pi)$ tends to zero as $t\to 1_+$ and achieves its maximum of $1/(3\pi)$ at $t=\pi/2$ when $U(\pi/2)=1$. For $t>\pi/2$, this rate decreases monotonically to zero as $t\to\infty$. Since the viscous solution approaches this (unique) weak solution in the limit $\nu\to 0$, the limiting energy dissipation rate for $t\ge 1$ is $U^3/(3\pi)$. The maximum dissipation rate corresponds to $U=1$, i.e., $\epsilon_m=1/(3\pi)$, occurring at $t=t_*=\pi/2$. Note that t_* differs from T and is the time for the extrema (initially at $x=\pm\pi/2$) to arrive at the stationary shock position $x=0$. In the next subsection, we recover both values of ϵ_m and t_* with high precision by numerical simulations.

An interesting feature of the present problem is that in the inviscid limit the energy commences its decay from $t=1$, while the maximum velocity does so from $t=\pi/2$, upon which the energy dissipation reaches its peak. This lag in the dissipation of $\|u\|_\infty$ can be readily appreciated by the following observation. For the energy, the dissipation rate is dominated by $|u_x(0,t)|$, which becomes sufficiently large at $t=1$, upon which the transition between nondissipative and dissipative phases takes place. For the maximum velocity, by taking the limit $p\to\infty$ of Eq. (7) we obtain

$$\frac{d}{dt}\|u\|_\infty = -\nu\lim_{p\to\infty}(p-1)\|u\|_p^{1-p}\langle |u|^{p-2}u_x^2\rangle. \tag{33}$$

The dissipation rate on the right-hand side of Eq. (33) is dominated by $|u_x|$ in the vicinity of the maximum velocity. Evidently, as the maximum velocity approaches the vertical axis, $|u_x|$ in its vicinity becomes greater (see Fig. 1). The transition between inviscid and viscous dynamics of $\|u\|_\infty$ at $t=\pi/2$ implies that $|u_x|$ in this vicinity is not sufficiently large until $t=\pi/2$. A similar behavior has been observed numerically in two-dimensional turbulence, whereby the vorticity supremum remains virtually unchanged until (and even after) the dissipation rate of the mean square vorticity has achieved its maximum value.[23]

The weak solution provides a convenient way for calculating the dissipation rate $d\|u\|_\infty/dt$ for $t\ge\pi/2$. In the limit

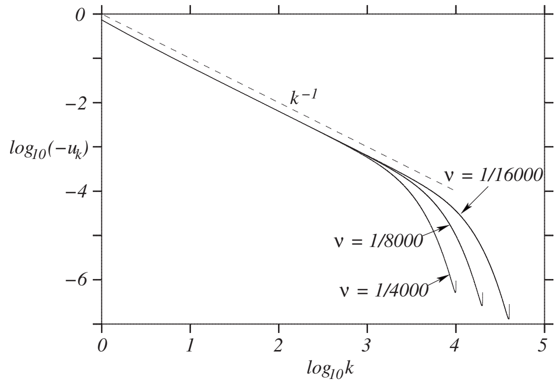

FIG. 3. Spectra ($-u_k$ vs k) at $t=\pi/2$ for the three smallest values of viscosity considered, $\nu=1/4000$, 1/8000, and 1/16000 (computed at resolutions $k_{\max}=10\,000$, 20 000, and 40 000, respectively). Note that the spectra differ negligibly, except in their high wave number tails, and are well fit by a k^{-1} slope in the inertial range.

$\nu\to 0$, one can identify $\|u\|_\infty$ with $U=\sin(Ut)$. By taking the time derivative of this expression and solving the resulting equation for $dU/dt=d\|u\|_\infty/dt$ we obtain

$$\frac{d}{dt}\|u\|_\infty = -\frac{\|u\|_\infty(1-\|u\|_\infty^2)^{1/2}}{1+t(1-\|u\|_\infty^2)^{1/2}}. \quad (34)$$

In the present example, $-u_x(x,0)$ peaks at an isolated point, namely at $x=0$. The weak solution is a step function with $U(T)=0$ and the energy dissipation rate tends to zero as $t\to T_+$. Similarly, consider a smooth initial profile $u(x,0)$ for which $-u_x(x,0)$ achieves a positive maximum at a finite number, say N_0, of isolated points. Such a profile evolves into a piecewise smooth solution having N_0 steps, each with $U(T)=0$. For this case, the energy dissipation rate also tends to zero as $t\to T_+$. When the said maximum occurs over an extended interval, say $[x_1,x_2]$, then $U(T)=(x_1-x_2)u_x(x_1,0) > 0$. The energy dissipation rate upon wave breaking jumps from zero to a positive value.

B. Numerical results

We now turn to results of a numerical analysis of the Burgers equation. We have simulated the initial value problem described by Eq. (28), where $u_1(0)=-1$ and $u_k(0)=0$ for $k>1$, for several different resolutions up to $k_{\max}=4\times 10^4$. For this given initial condition and $c=\sqrt{3}$, Eq. (22) becomes $D\le\sqrt{3}/\nu$. The viscosity $\nu=2.5/k_{\max}$ has been chosen in accord with this estimate to ensure that $k_{\max}$ lies well within the dissipation range. Our choice turns out to yield adequate dissipation, thus providing evidence for the sharpness of Eq. (22). We have used a standard fourth order Runge–Kutta method with the viscosity exactly incorporated through an integrating factor. The adapted time step $\delta t=-0.01/\Sigma_k k u_k$ has been used to account for the highly sensitive nature of the problem when $t\approx t_*$.

Figure 3 shows the plots of $\log[-u_k(t_*)]$ versus $\log k$ for the three highest-resolution simulations. These exhibit a clear slope of -1 in the inertial range, thus implying the scaling k^{-2} for the energy spectrum. Evidently, the inertial range becomes wider for higher Re and a careful inspection of data

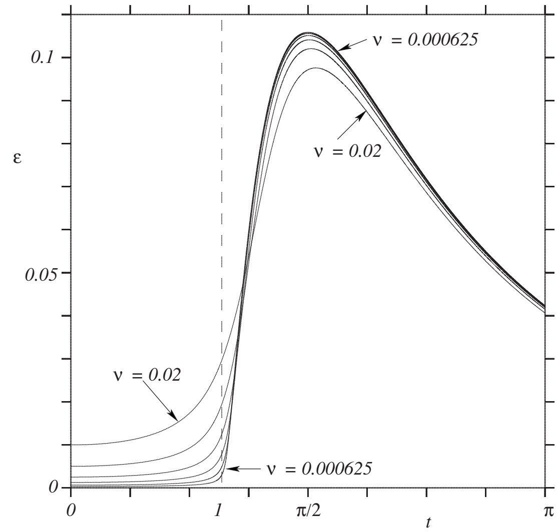

FIG. 4. Evolution of the energy dissipation rate $\epsilon(t)$ for a series of six simulations differing in ν by factors of 2 (the extreme values of ν are indicated). Also, the inviscid singularity time ($t=1$) is indicated by the vertical dashed line.

also shows a clear trend that the inertial range becomes shallower, approaching the critical scaling k^{-1} as expected.

Figure 4 shows the evolution of the energy dissipation rate $\epsilon(t)=\nu\|u_x\|^2=\nu\Sigma_k k^2u_k^2/2$ from $t=0$ to $t=\pi$. The dissipation rate remains small for $t<1$ (evidently tending to zero in the inviscid limit), only to grow considerably when $t=1$, consistent with the result (32) for the limiting weak solution. This rate continues to increase for $t>1$ and achieves a maximum at $t=t_*=1.571$, which is very close to the analytic value $\pi/2$. This value of t_* has been observed to be very robust with respect to independent variations of the Reynolds number and the time step. The maximum dissipation rate is $\epsilon_m=0.106\,05$ for the three highest Reynolds numbers. This suggests that the convergence of ϵ_m as $\nu\to 0$ is rapid. Indeed, Fig. 5 shows that ϵ_m differs only by approximately 0.39ν from the theoretical limiting value $1/(3\pi)$. The curve in this

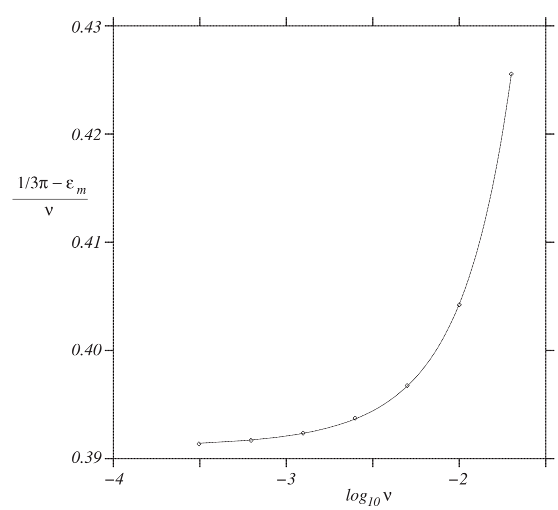

FIG. 5. Least-squares quadratic fit $[1/(3\pi)-\epsilon_m]/\nu=0.3911+0.9102\nu+40.50\nu^2$ to the numerical results indicated by the diamonds.

figure shows the least-squares quadratic fit $[1/(3\pi)-\epsilon_m]/\nu = 0.3911+0.9102\nu+40.50\nu^2$ to the numerical results indicated by the diamonds.

We now discuss the results from a second set of simulations, differing from the first only in the initial condition: $u_2(0)=-1$ and $u_k(0)=0$ for $k\neq 2$. In physical space this corresponds to $u(x,0)=-\sin 2x$. For this case, only even wave numbers can be excited. Initially, the steepest slope is -2 occurring at $x=\pm\pi,0$, where the inviscid solution blows up simultaneously when $t=T=1/2$. One would expect ϵ_m to be twice as great as that in the previous case because the combined contribution to ϵ_m at both $x=-\pi$ and $x=\pi$ is equivalent to that at $x=0$. Furthermore, since the local extrema are $\pi/4$ away from the (stationary) locations of wave breaking, one would expect $t_*=\pi/4$. These are actually what we have observed. More precisely, the numerics have returned $\epsilon_m=0.2121$ and $t_*=0.7856$. The spectrum plot is the same as Fig. 3 and is not shown.

In passing, it is worth mentioning that for the present example, ϵ_m can be made arbitrarily large by changing the initial condition. Given $u_\ell(0)=-1$ and $u_k(0)=0$ for $k\neq\ell$, which corresponds to $u(x,0)=-\sin \ell x$ in physical space, only the wave numbers $\ell, 2\ell, 3\ell, \cdots$ can be excited. Initially, the steepest slope is $-\ell$ occurring at $x=2\pi n/\ell$ for $n=0,\pm 1,\pm 2,\cdots$ and $|n|\leq \ell/2$, where the inviscid solution blows up simultaneously when $t=T=1/\ell$. The local extrema are $\pi/(2\ell)$ away from the (stationary) locations of wave breaking. One can expect $\epsilon_m=\ell/(3\pi)$ and $t_*=\pi/(2\ell)$, which we have actually observed (within small errors as the cases reported above) for several different values of ℓ. Note that although ϵ_m can be made arbitrarily large by increasing ℓ, Eq. (14) does hold as both of its sides are proportional to ℓ ($k_0=\ell/L$). The scaling $E(k,t_*)=Ck^{-2}$, starting from $k=\ell$, has been observed to prevail for all cases, with $C\propto\ell$.

V. CONCLUSION

In summary, we have studied both analytically and numerically one-dimensional viscous Burgers flows decaying from smooth initial conditions. The results obtained include upper bounds for the energy dissipation rate and number of degrees of freedom and constraints on the spectral distribution of energy. Given that the maximally achievable energy dissipation rate ϵ_m remains finite and positive in the inviscid limit $\nu\to 0$, it is found that energy spectra steeper than k^{-2} are ruled out in that limit. For this critical scaling, ϵ_m satisfies $\epsilon_m\leq\sqrt{3}k_0\|u_0\|_\infty\|u_0\|^2$, where k_0 is the lower wave number end of the energy inertial range and u_0 is the initial velocity field. This further implies the upper bound $k_\nu\leq\sqrt{3}\|u_0\|_\infty/\nu$ for the energy dissipation wave number k_ν. It follows that the number N of Fourier modes within the energy inertial range satisfies $N\leq\sqrt{3}L\|u_0\|_\infty/\nu$, where L is the domain size. This result coincides with a rigorous estimate, using no assumption of power-law spectra, for the number of degrees of freedom D defined in terms of local Lyapunov exponents.

As an illustrative example, we have considered both analytically and numerically the Burgers equation in the periodic domain $[-\pi,\pi]$ with the initial condition $u_0(x)=-\sin x$. In the former approach, we have tightened up the constraint on the spectral distribution of energy by pointing out that no power-law energy spectra other than k^{-2} are realizable. A detailed examination of the (unique) limiting weak solution has provided an explanation why the maximum velocity is better conserved than the energy. In the latter approach, we have demonstrated the exact k^{-2} scaling and have numerically determined the viscosity-independent dissipation rate and time of maximum energy dissipation. These are consistent with analytic results derived from the limiting weak solution.

[1] J. M. Burgers, "A mathematical model illustrating the theory of turbulence," Adv. Appl. Mech. **1**, 171 (1948).
[2] E. Hopf, "The partial differential equation $u_t+uu_x=\mu u_{xx}$," Commun. Pure Appl. Math. **3**, 201 (1950).
[3] J. D. Cole, "On a quasi-linear parabolic equation occurring in aerodynamics," Q. Appl. Math. **9**, 225 (1951).
[4] J. Bec and U. Frisch, "Probability distribution functions of derivatives and increments for decaying Burgers turbulence," Phys. Rev. E **61**, 1395 (2000).
[5] J. Bec, U. Frisch, and K. Khanin, "Kicked Burgers turbulence," J. Fluid Mech. **416**, 239 (2000).
[6] A. Chekhlov and V. Yakhot, "Kolmogorov turbulence in a random-force-driven Burgers equation," Phys. Rev. E **51**, R2739 (1995).
[7] W. E and E. Vanden Eijnden, "On the statistical solution of the Riemann equation and its implication on Burgers turbulence," Phys. Fluids **11**, 2149 (1999).
[8] W. E and E. Vanden Eijnden, "Another note on forced Burgers turbulence," Phys. Fluids **12**, 149 (2000).
[9] T. Gotoh and R. H. Kraichnan, "Steady-state Burgers turbulence with large-scale forcing," Phys. Fluids **10**, 2859 (1998).
[10] V. H. Hoang and K. Khanin, "Random Burgers equation and Lagrangian system in non-compact domains," Nonlinearity **16**, 819 (2003).
[11] M. Vergassola, B. Dubrulle, U. Frisch, and A. Noullez, "Burgers-equation, devils staircases and the mass-distribution for large-scale structures," Astron. Astrophys. **289**, 325 (1994).
[12] V. Yakhot and A. Chekhlov, "Algebraic tails of probability functions in the random-force-driven Burgers turbulence," Phys. Rev. Lett. **77**, 3118 (1996).
[13] R. V. Y. Nguyen, M. Farge, D. Kolomensky, K. Schneider, and N. Kingsbury, "Wavelets meet Burgulence: CVS-filtered Burgers equation," Physica D **237**, 2151 (2008).
[14] C. V. Tran, "Constraint on scalar diffusion anomaly in three-dimensional flows having bounded velocity gradients," Phys. Fluids **20**, 077103 (2008).
[15] J. Kaplan and J. Yorke, *Functional Differential Equations and Approximation of Fixed Points* (Springer, New York, 1979), p. 228.
[16] J. D. Farmer, "Chaotic attractors of an infinite-dimensional dynamical system," Physica D **4**, 366 (1982).
[17] C. V. Tran and L. Blackbourn, "Number of degrees of freedom of two-dimensional turbulence," Phys. Rev. E **79**, 056308 (2009).
[18] C. V. Tran, "The number of degrees of freedom of three-dimensional Navier–Stokes turbulence," Phys. Fluids **21**, 125103 (2009).
[19] C. V. Tran, D. G. Dritschel, and R. K. Scott, "Effective degrees of nonlinearity in a family of generalized models of two-dimensional turbulence," Phys. Rev. E **81**, 016301 (2010).
[20] M. C. Cross and P. C. Hohenberg, "Pattern formation outside of equilibrium," Rev. Mod. Phys. **65**, 851 (1993).
[21] P. C. Hohenberg and B. I. Shraiman, "Chaotic behaviour of an extended system," Physica D **37**, 109 (1989).
[22] C. V. Tran, T. G. Shepherd, and H.-R. Cho, "Extensivity of two-dimensional turbulence," Physica D **192**, 187 (2004).
[23] D. G. Dritschel, C. V. Tran, and R. K. Scott, "Revisiting Batchelor's theory of two-dimensional turbulence," J. Fluid Mech. **591**, 379 (2007).